



## Adsorption of heavy metals using activated carbon produced from municipal organic solid waste

Muhammad H. Al-Malack\*, Abdullah A. Basaleh

*Department of Civil and Environmental Engineering, King Fahd University of Petroleum and Minerals, Box 1150, Dhahran 31261, Saudi Arabia, Tel. +966 138604735; Fax: +966 138602789; emails: mhmack@kfupm.edu.sa (M.H. Al-Malack), g201102170@kfupm.edu.sa (A.A. Basaleh)*

Received 21 October 2015; Accepted 9 January 2016

### ABSTRACT

Adsorption of cadmium ( $\text{Cd}^{2+}$ ) and lead ( $\text{Pb}^{2+}$ ) was investigated using activated carbon (AC) produced from municipal organic solid waste (MOSW). The produced AC was characterized using Scanning Electron Microscopy, X-ray Diffraction, Fourier Transform Infrared spectroscopy, and Brunauer–Emmett–Teller. The results showed that an AC with a surface area of  $790 \text{ m}^2/\text{g}$  was produced at carbonization temperature and time of  $700^\circ\text{C}$  and 2 h, respectively, and activation with phosphoric acid concentration of 30%. The effect of operational factors, namely, pH 3–7, contact time (0–480 min), metal concentration (25–300 mg/L), and adsorbent dosage (25–300 mg per 50 mL of metal solution) on the adsorption process was investigated. The results showed that optimum adsorption of  $\text{Cd}^{2+}$  and  $\text{Pb}^{2+}$  were obtained at pH of 5, contact time of 180 min, metal concentration of 100 mg/L, and adsorbent dose of 200 mg per 50 mL of metal solution. At optimum operational conditions, removal efficiencies of 78 and 94% for  $\text{Cd}^{2+}$  and  $\text{Pb}^{2+}$ , respectively, were achieved. The isotherms also showed that the maximum adsorption capacity of  $\text{Cd}^{2+}$  and  $\text{Pb}^{2+}$  were 61 and 90 mg/g, respectively, at equilibrium time of 120 min and pH value of 5.

*Keywords:* Isotherms; Kinetic models; BET; XRD; FTIR; SEM

### 1. Introduction

Due to large industrial activities such as electroplating, mining, and car manufacturing, large quantities of heavy metals are being discharged to water bodies on daily basis. Beside their toxicity, heavy metals are non-biodegradable and accumulate in food chain and human tissues that may result in serious health and environmental problems [1]. Consequently, control of metal concentrations discharged to surrounding environments is an indispensable process. Various

treatment technologies such as ion exchange [2], electrochemical treatment [3], chemical precipitation [4], and forward osmosis [5] were used in the removal of metals. However, some treatment processes are either expensive or possess several limitations. Advantages and drawbacks of treatment processes have been widely discussed by Barakat [6]. Due to its simplicity in design and operation; and applicability in the removal of numerous contaminants, adsorption is considered as one of the most widely used techniques in wastewater treatment [7]. Recently, great number of researchers used activated carbon (AC) to remove several pollutants, including metals [8] and phenols and

\*Corresponding author.

dyes [9]. Due to its high surface area and removal efficiency, AC is one of the most common adsorbents used to remove heavy metals from water and wastewater. Nevertheless, its use is limited due to high production cost of commercial AC; therefore, the search for alternative low-cost sources of AC is highly encouraged. Various types of agricultural waste materials such as rice husk [10], wheat straw [11], orange peel [12], banana peel [13], and pomegranate peel [14] have been utilized as potential low-cost sources of AC with and without activation. Recently, Mahajan et al. [15] investigated the use of orange peel as adsorbent for the removal of Mg, Cu, Mn, and Zn from winery wastewater. The maximum adsorption efficiencies of Cu, Zn, Mn, and Mg were reported to be 33.35, 30.26, 31.92, and 47.5%, respectively. Inactivated orange peel was also studied for the removal of Ni from aqueous solutions by Gönen and Serin [16]. The effects of operational factors such as temperature, time, adsorbent dosage, and pH were investigated. The maximum adsorption capacity of Ni was found to be 62.3 mg per gram of adsorbent at a pH value of 5.0. Moreover, without chemical activation, banana and orange peels were investigated as potential inexpensive biosorbents to remove  $Pb^{2+}$ ,  $Cu^{2+}$ ,  $Zn^{2+}$ ,  $Ni^{2+}$ , and  $Co^{2+}$  from synthetic solutions by Annadurai et al. [17]. Maximum adsorption capacities for both banana and orange peels were reported in the following order  $Pb^{2+} > Ni^{2+} > Zn^{2+} > Cu^{2+} > Co^{2+}$ , where maximum adsorption capacities of orange peel were 7.75, 3.65, 5.25, 6.01, and 1.82 mg/g, respectively. For banana peel, maximum adsorption capacities were 7.97, 4.75, 5.8, 6.88, and 2.55 mg/g for  $Pb^{2+}$ ,  $Cu^{2+}$ ,  $Zn^{2+}$ ,  $Ni^{2+}$ , and  $Co^{2+}$ , respectively. Kadirvelu et al. [18] investigated the preparation of AC from banana pith for the removal of  $Hg^{2+}$  and  $Ni^{2+}$  from aqueous solutions. The results revealed that at optimum pH value of 5.0, the maximum removal efficiency of  $Hg^{2+}$  and  $Ni^{2+}$  was 100 and 96.40%, respectively, which was achieved after 24 h of contact time. AC derived from pomegranate peel was used to remove  $Cu^{2+}$  and  $Pb^{2+}$  from aqueous solutions by El-Ashtoukhy et al. [19]. They reported that maximum removal efficiencies were 97 and 92% for  $Cu^{2+}$  and  $Pb^{2+}$ , respectively. Moreover, adsorption of  $Cu^{2+}$  by potato peel was investigated by Aman et al. [20], where carbonization was performed at a temperature of 700°C. The results showed that a removal efficiency of 98.8% of  $Cu^{2+}$  was achieved. In addition to agricultural waste materials, few studies investigated the use of mixed waste materials in AC production. AC was prepared from three waste materials; paper, plastic, and palm by Habila et al. [21]. Equal weight ratios of waste materials were mixed, carbonized, and activated using Ca(OH). The produced AC was used to adsorb

Tartrazine dye, where maximum adsorption capacity of 74.9 mg/g was reported.

The published literature reported several methods that were used to produce AC with high surface area, consequently, preparation method as well as carbon precursor play key role in microporosity of produced AC. Fundamentally, preparation of AC consists of two major processes, namely, carbonization and activation of raw materials. Carbonization is the process through which non-carbon elements are removed from raw materials whereas carbon content is increased at high temperatures, which usually vary between 400 and 800°C [22]. Generally, activation process occurs after carbonization process. The main purpose of activation is to increase internal surface area and develop porosity, which in turn increases the sorption capacity of carbonized materials. Two distinct activation methods were reported in the published literature, namely, physical and chemical activation. In physical activation processes, reaction occurs between carbon and an oxidizing gas such as oxygen, carbon dioxide, or carbon monoxide. On the other hand, in chemical activation, carbon reacts with chemical activating agents such as  $ZnCl_2$ , KOH,  $H_3PO_4$ , and  $K_2CO_3$ .

The extensive literature review revealed that the use of single waste materials in AC production is very well documented. However, up to the knowledge of the investigators there is a lack of information regarding the utilization of randomly mixed waste materials, particularly, municipal organic solid waste (MOSW) in the production of AC. Accordingly, the main objective of the current research is to investigate the potentiality of utilizing MOSW as an inexpensive source of AC. Chemical activation process using  $H_3PO_4$  and KOH as activating agents will be implemented for the production of the AC. The produced AC will be utilized to remove  $Cd^{2+}$  and  $Pb^{2+}$  individually from synthetic aqueous solutions. The selection of  $Cd^{2+}$  and  $Pb^{2+}$  was due to their common presence in industrial wastewater.

## 2. Materials and methods

### 2.1. Raw material

MOSW was collected randomly from different houses. The collected MOSW composed mainly of varying quantities of the following materials; orange and lemon peels (13.1%), banana peels (6.1%), mango peels and stones (3.1%), melon and watermelon shells (2%), potato peels, onion and garlic shells (5.3%), plant stalks (16.8%), bread crumbs (21.17%), fish and animal bones (4.81%), and others (27.5%). The collected MOSW was well-mixed, washed thoroughly with distilled water to remove any physically adhered

materials and dried in an air oven at 110°C for 24 h. The dried MOSW was then comminuted using FRITSCH Pulverisette 19 universal cutting mill to obtain a final particle size of about 0.4 mm.

## 2.2. Production of AC from MOSW

To produce AC, 10 g of the comminuted MOSW were mixed thoroughly with 20 ml of H<sub>3</sub>PO<sub>4</sub> solution (30% w/w). The impregnation process was performed at room temperature for 1 h. Impregnated samples were dried overnight in a heating/drying oven (Fisher Scientific) at 110°C. The slurry was then placed inside stainless steel tubes of 300-mm length and 50-mm diameter. The tubes have two 8-mm diameter ports and two removable lids at both ends. The tubes were then placed inside a muffle furnace (EURO THERM) that was heated at slow rate (5°C/min) up to a holding temperature of 700°C in order to allow free evolution of volatiles. The process was performed at optimum conditions of temperature (700°C) and time (2 h). The produced AC was cooled and repeatedly washed with hot distilled water to remove residual traces of the activating agent. When pH values of the washing water was close to neutral, the washing process was considered complete. After washing, samples were placed in a heating/drying oven (Fisher Scientific) at 110°C for 24 h. Finally, the produced AC was grounded and sieved to particle size of less than 0.30 mm.

## 2.3. Characterization of the AC samples

In order to characterize the produced AC, the following standard procedures were employed.

### 2.3.1. Yield

Yield of the produced AC was calculated using the following formula:

$$\text{Yield(\%)} = \frac{\text{weight of produced activated carbon}}{\text{weight of raw material (MOSW)}} \quad (1)$$

### 2.3.2. Surface chemistry

Fourier Transform Infrared spectroscopy (FT-IR) technique was applied to determine surface functional groups of the raw material (MOSW) and produced AC samples using the Thermo Electron Corporation Nicolet Nexus 670 FT-IR Spectrometer. Moreover, the

KBr pellet was used to record the transmission spectra of MOSW and produced AC samples.

### 2.3.3. Microscopy

Scanning Electron Microscope (SEM), using JEOL 5800 LV, was utilized to examine the surface morphology of raw material (MOSW) and produced AC samples. Energy Dispersive Spectrometer (EDS) was used to investigate the elemental surface composition of MOSW and produced AC samples.

### 2.3.4. X-ray diffraction spectroscopy

Crystalline structures of raw material (MOSW) and produced AC samples were examined using X-ray diffraction technique (XRD), where Ultima IV X-ray diffractometer was used. Scan runs were conducted at angles ranging between 10° and 80°, with a step size of 0.02°/s.

### 2.3.5. Porosity characterization

Porous characteristics of the produced AC samples such as specific surface area, pore size, and pore volume were investigated using standard multi point BET method [23]. Nitrogen gas (N<sub>2</sub>) adsorption isotherms at 77° K were conducted on the prepared samples using an automatic adsorption unit (Micrometric, ASAP 2020 V3.05 H).

## 2.4. Adsorption experiments

Single adsorption experiments of Cd<sup>2+</sup> and Pb<sup>2+</sup> in batch mode were conducted in order to evaluate the adsorption capacity of the produced AC. Stock solutions of 1,000 mg/L of Cd<sup>2+</sup> and Pb<sup>2+</sup> were prepared from nitrate salts by dissolving 2.744 g and 1.5984 g of Cd(NO<sub>3</sub>)<sub>2</sub>·4H<sub>2</sub>O and Pb(NO<sub>3</sub>)<sub>2</sub> (BDH Laboratory supplies), respectively, in 500 ml of deionized water. Before making up to 1,000 ml, stock solutions were acidified to a pH value of less than 2.0 using HNO<sub>3</sub>. Different amounts of the produced AC were added to 50-ml volumes of metal solutions having different concentrations of Cd<sup>2+</sup> and Pb<sup>2+</sup> and shook at 200 rpm for different times. At the end of shaking times, samples were filtered and acidified to make them ready for metal analysis. Atomic Absorption Spectroscopy (PerkinElmer Analyst 700-AAS) was used to measure concentrations of metal ions before and after treatment. Each experiment was carried out in duplicate in order to obtain reliable results. Moreover, blank samples

were used, where produced AC was not added to the synthetic wastewater. Effects of initial concentration, adsorbent dosage, pH, and contact time on the performance of the adsorption process were investigated.

### 3. Results and discussion

#### 3.1. BET surface area characterization and chemistry

##### 3.1.1. BET surface area characterization

The N<sub>2</sub> adsorption isotherms at 77 K showed that the prepared AC has porous characteristics as illustrated in Table 1. As shown in the table, the BET surface area of the produced AC is 792.93 m<sup>2</sup>/g. Also, porosity was developed with average pore width (*D<sub>p</sub>*) of about 26.4 Å (2.64 nm). It is worth mentioning that production yield of the AC from MOSW was 32% at optimum conditions of carbonization and activation processes.

##### 3.1.2. Surface chemistry

FTIR spectra of MOSW and produced AC samples were reported within 500–4,000 cm<sup>-1</sup> as shown in Fig. 1. The results showed that almost the same functional groups were found in both samples, which clearly indicate that the activation process has mainly enhanced the porosity of the AC and made insignificant changes to the surface chemistry. Similar results were reported by El-Hendawy et al. [24], who produced AC from cotton stalks with phosphoric acid. Moreover, Fig. 1 revealed the presence of different functional groups including oxygen, amines, and unsaturated hydrocarbons. In the case of MOSW, the presence of hydroxyl with high intensity broad peak was observed at 3,447 cm<sup>-1</sup>, where similar results were reported at 3,448 cm<sup>-1</sup> by El-Hendawy [25]. Sharp peaks at 2,895 and 2,925 cm<sup>-1</sup> could be attributed to the presence of symmetric and asymmetric C–H methylene and methyl groups, respectively [24]. The strong band at wave number of 1,745 cm<sup>-1</sup> is attributed to the presence of carbonyl ester group (C=O). This band was also observed at wave numbers of 1,742 and 1,745 cm<sup>-1</sup> by El-Hendawy et al. and El-Hendawy, respectively [24,25]. The strong band at 1,645 cm<sup>-1</sup> might be attributed to the presence of C=C

alkane group, while the medium band at 1,416 cm<sup>-1</sup> might be ascribed to the presence of C–H bending of methylene group. The strong bands at around 1,150 and 1,080 cm<sup>-1</sup> could be attributed to the presence of C–O alcohol and ester stretching group, respectively, while the strong band stretch C–H group was observed at low wave number of 670 cm<sup>-1</sup>. Fig. 1 shows that the main difference between MOSW and produced AC samples was the weak intensities of different waves of the produced AC when compared to the MOSW. This could be attributed to the effect of phosphoric acid impregnation and high carbonization temperatures. During the activation process at high temperatures, there is an increase in volatile matter due to carbonization and aromatization, which results in destructing the chemical bonds that may lead to weak intensities [24,25]. Sharp decrease in band intensities of AC prepared from cotton stack was observed by El-Hendawy et al. [24]. In the current investigation, AC was produced using H<sub>3</sub>PO<sub>4</sub> at 700 °C.

Weak intensities of AC spectra due to the carbonization and aromatization were confirmed by the presence of strong band at 1,745 cm<sup>-1</sup> in MOSW sample, which was shifted to 1,740 cm<sup>-1</sup> and became very weak in the produced AC sample. El-Headway [25], who prepared AC from date pits using 50% H<sub>3</sub>PO<sub>4</sub> also noticed the appearance of band 1,742 cm<sup>-1</sup> in raw material and its absence in the produced AC sample. In addition, El-Hendawy et al. [24] observed the presence of band 1,745 in raw material (cotton stalk) while it was absent in the produced AC. It is clear that in the previous studies the bands around 1,745 cm<sup>-1</sup> disappeared, while it was very weak in the current study, which could be attributed to the difference in the concentration of H<sub>3</sub>PO<sub>4</sub> that was used in the activation process. In the current study, the MOSW was impregnated with 30% of H<sub>3</sub>PO<sub>4</sub> while 50% of the same acid was used by El-Headway et al. [24]. Furthermore, group C=C at 1,646 cm<sup>-1</sup> in MOSW sample was found to shift to 1,590 cm<sup>-1</sup> and looked weaker in the produced AC sample. This might be ascribed to the condensation of aromatic group during the activation process. Similar findings were also observed by El-Hendawy et al. [24], where the wave number was found to shift from 1,600 cm<sup>-1</sup> in the raw material to 1,575 cm<sup>-1</sup> in the produced AC. Moreover, the C–H group was observed to shift from 1,416 cm<sup>-1</sup> (in the

Table 1  
Surface area and porosity characteristics of produced AC

BET (m <sup>2</sup> /g)	S <sub>ext</sub> (m <sup>2</sup> /g)	S <sub>mic</sub> (m <sup>2</sup> /g)	V <sub>t</sub> (cm <sup>3</sup> /g)	V <sub>mic</sub> (cm <sup>3</sup> /g)	D <sub>p</sub> (Å)
792.93	419.28	373.65	0.523	0.192	26.40

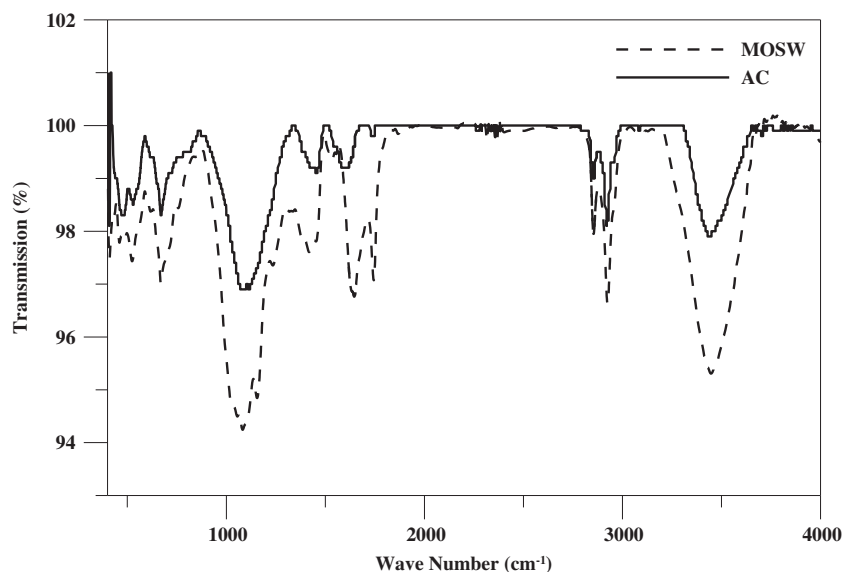


Fig. 1. FT-IR spectra of raw material (MOSW) and produced AC samples.

MOSW sample) to  $1,450\text{ cm}^{-1}$  (in the produced AC sample), which could be attributed to the formation of C=C. The strong bands at around  $1,150$  and  $1,080\text{ cm}^{-1}$  in the spectra of the produced AC may be ascribed to the formation of linear and cyclic polyphosphate ester group P=O due to treatment with phosphoric acid. This is consistent with the increase in the content of phosphorus in the surface of the produced AC when compared to the MOSW sample as shown in the results of the SEM analysis. These results are in good agreement with those reported by other researchers [24,25]. Fernandez et al. [12] who investigated the FT-IR spectra of AC samples prepared from orange peels with 50 (weight percent) phosphoric acid reported the presence of P–O functional group at  $1,070\text{ cm}^{-1}$ .

### 3.1.3. Microscopy

Table 2 shows the elemental surface composition of MOSW and produced AC. Three local spots were investigated and the minimum, average, and maximum values are presented. The table clearly shows that the main components of both MOSW and produced AC are carbon, oxygen, and small amounts of calcium, potassium, phosphorus, and chloride. The results revealed that during the activation process, non-carbonaceous materials were removed, which was consistent with the increase in carbon content from around 64.4% in MOSW to 82.4% in the produced AC and the absence or sharp decrease of other metals in the elemental analysis of the produced AC. Moreover,

phosphorus content increased from around 0.30% in MOSW to around 4.6% in the produced AC, which can be attributed to impregnation with phosphoric acid. Furthermore, Table 2 shows that surface of the produced AC is rich in oxygen and phosphorus functional groups, which is consistent with the results obtained by the FT-IR analysis of the produced AC surface. SEM micrographs of MOSW and the produced AC samples are depicted in Fig. 2, where the formation of different pores due to activation process is easily shown. The micrographs also show the heterogeneity of the produced AC surface and the irregular distribution of pores.

### 3.1.4 X-ray diffraction spectroscopy analysis

Crystalline structures of MOSW and the produced AC were examined by XRD. Patterns of XRD of MOSW and the produced AC are shown in Fig. 3. The figure clearly shows that no sharp peaks were observed, while broad peaks indicate that the structure is amorphous and non-graphitizing, therefore, good porous structure can be developed [26]. In MOSW, the broad peak at  $2\theta = 23^\circ$  might be attributed to the typical silica characteristics. This peak disappeared in the spectra of the produced AC, which can be attributed to ash removal due to heat and acid treatment during the activation process. Similar findings were reported by Liou [27], who prepared AC from biomass using phosphoric acid and zinc chloride. He reported that the same peak was observed in the spectra of the raw material while it was absent in the

Table 2  
Localized spot elemental analysis of MOSW and AC samples

Local spot	C (%)	O (%)	Ca (%)	K (%)	Cl (%)	P (%)
<i>MOSW</i>						
Spot 1	64.6	32.7	1.8	0.6	0.3	0.2
Spot 2	63.1	33.2	2.2	0.7	0.3	0.6
Spot 3	65.5	32	1.3	0.5	0.2	0.2
Max	65.5	33.2	2.2	0.7	0.3	0.6
Min	63.1	32	1.3	0.5	0.2	0.2
Average	64.4	32.6333	1.76667	0.6	0.26667	0.33333
<i>AC</i>						
Spot 1	82.7	12.0	0.60			4.7
Spot 2	81.6	12.4	0.50			4.4
Spot 3	83.0	11.8	0.50			4.7
Max	83.0	12.4	0.60			4.7
Min	81.6	11.8	0.50			4.4
Average	82.4	12.1	0.53			4.6

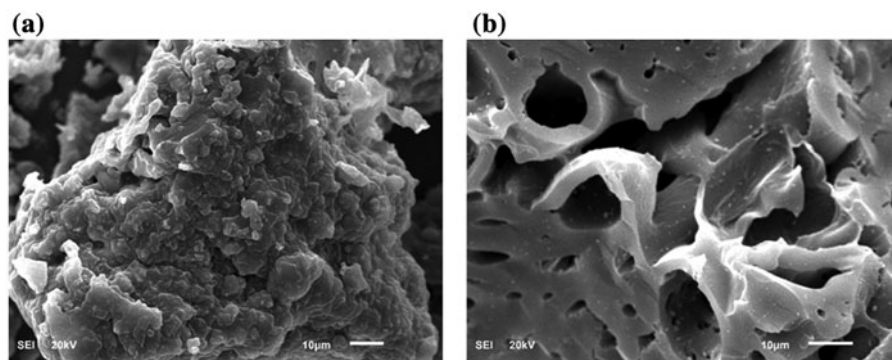


Fig. 2. SEM micrographs of (a) MOSW and (b) AC samples.

spectra of the produced AC. As shown in Fig. 3, the presence of broad peaks at  $2\theta \approx 26^\circ$  and  $43^\circ$  in the XRD of the produced AC indicates that better alignment of crystalline structure was formed. This was also reported by Tongpoothorn et al. [28] who prepared AC from *Jatropha curcas* fruit shell. In addition, these two peaks ( $2\theta \approx 26^\circ$  and  $43^\circ$ ) might be ascribed to the presence of particular graphite and sodalite or mullite, respectively. Similar peaks were observed and reported by Salehin et al. [29], where XRD of AC produced from residual oil fly ash was investigated.

### 3.2. Effect of operational factors

#### 3.2.1. Effect of pH

The effect of pH on the adsorption of  $\text{Cd}^{2+}$  and  $\text{Pb}^{2+}$  was investigated at pH values of 3, 4, 5, 5.5, 6, and 7. The above-mentioned pH values were selected

due to the fact that at pH values higher than 7, precipitation of metal ions may occur [30]. The pH effect was investigated at initial metal concentration of 100 mg/L, adsorbent dosage of 50 mg, contact time of 3 h, solution volume of 50 mL, shaking speed of 200 rpm. Fig. 4 shows the effect of pH on the removal efficiency of  $\text{Cd}^{2+}$  and  $\text{Pb}^{2+}$ . Isotherms were conducted in duplicates and only average results were reported in the figure. The results clearly show that by increasing pH values, removal efficiencies of both  $\text{Cd}^{2+}$  and  $\text{Pb}^{2+}$  were also found to increase. When pH values were increased from 3 to 7, the removal efficiency increased from 26.5 to 38% and from 50 to 85% for  $\text{Cd}^{2+}$  and  $\text{Pb}^{2+}$ , respectively. This is attributed to the fact that at lower pH values, there is strong competition between hydrogen ions ( $\text{H}^+$ ) and metal ions for AC surface sites, which resulted in lower removal efficiencies. However, when pH values were increased, the competition decreased due to the decrease in  $\text{H}^+$

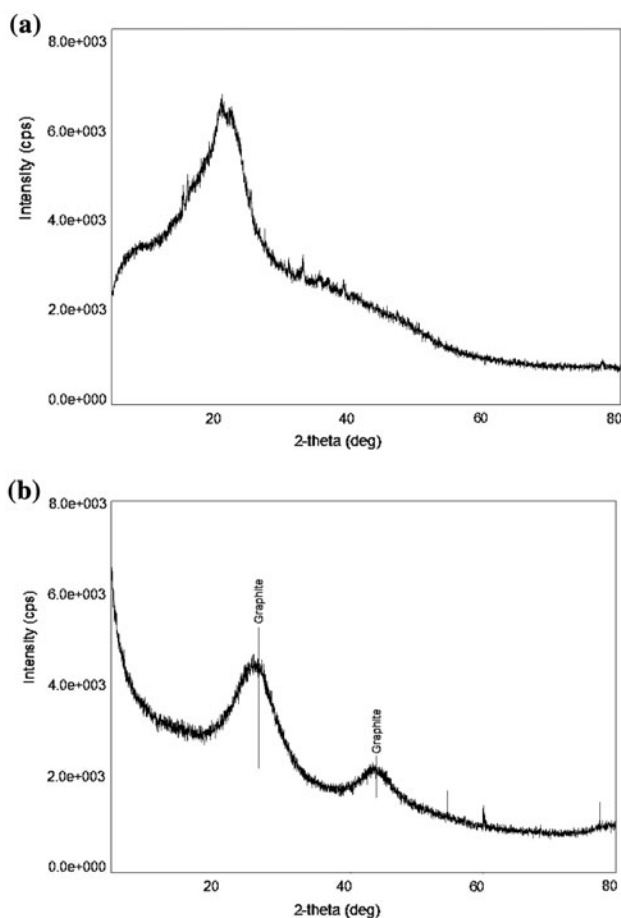


Fig. 3. XRD of (a) MOSW and (b) AC samples.

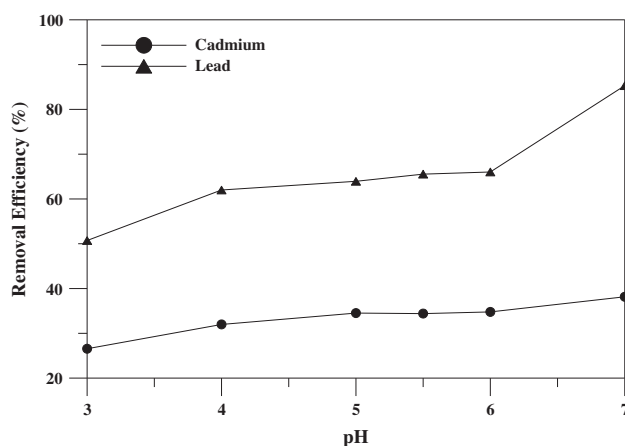


Fig. 4. Effect of pH on adsorption of  $\text{Cd}^{2+}$  and  $\text{Pb}^{2+}$  using produced AC.

and increase in  $\text{OH}^-$  [31,32]. Moreover, Taty-Costodes et al. [33] investigated the effect of pH on the removal efficiency of cadmium and lead by sawdust, where

similar results were reported. Moreover, the figure clearly demonstrates that when pH values were increased from 3 to 5, the removal efficiency of  $\text{Cd}^{2+}$  and  $\text{Pb}^{2+}$  was found to increase, however, the removal efficiency was not found to change significantly at pH values between 5 and 6. Moreover, when pH values were increased from 6 to 7, the removal efficiency was found to increase dramatically, particularly in the case of  $\text{Pb}^{2+}$ . This could be attributed to the fact that both adsorption and precipitation of metal ions as hydroxide may take place at pH values more than 6. This was confirmed by results obtained from blank samples at pH values between 3 and 7, where metal precipitation was very clear at pH values of more than 6. Based on that and in order to avoid metal precipitation, optimum pH value was selected as 5. These results are in agreement with those reported by investigators who studied the removal of cadmium and lead using AC produced from different raw materials [33,34]. Furthermore, the results showed that the removal efficiency of  $\text{Pb}^{2+}$  was found higher than that of  $\text{Cd}^{2+}$ , which could indicate that the produced AC prefers  $\text{Pb}^{2+}$  ions. This could be attributed to differences in metal properties, particularly the electronegativity, where lead has higher electronegativity (2.33) than cadmium (1.69), as shown in Table 3. In fact, metals with higher electronegativity values have stronger attachment to AC surfaces. In addition to the higher electronegativity and ionic radius,  $\text{Pb}^{2+}$  has lower hydrated radius when compared to  $\text{Cd}^{2+}$ ; consequently,  $\text{Pb}^{2+}$  can reach microspores of the produced AC faster than  $\text{Cd}^{2+}$ . Qin et al. [35] who studied the adsorption of cadmium, lead, and copper on peat reported that  $\text{Pb}^{2+}$  and  $\text{Cd}^{2+}$  were having the highest and lowest removal efficiencies, respectively, which was attributed to the differences in electronegativity, ionic radius, and hydrated ionic radius.

### 3.2.2. Effect of contact time

To investigate the effect of contact time on the removal efficiency of individual  $\text{Cd}^{2+}$  and  $\text{Pb}^{2+}$  using the produced AC, batch isotherm experiments were performed at different contact times (5–480 min), pH of 5, initial metal concentration of 100 mg/L, and

Table 3  
Properties of investigated metals ( $\text{Cd}^{2+}$  and  $\text{Pb}^{2+}$ )

Property	Lead	Cadmium
Electronegativity (Pauling)	2.33	1.69
Hydrated ionic radius (Å)	4.01	4.26
Ionic radius (Å)	1.19	0.95

adsorbent dosage of 50 mg per 50 mL of metal solution. Fig. 5 shows the removal efficiency of  $\text{Cd}^{2+}$  and  $\text{Pb}^{2+}$  with respect to time. Isotherms were conducted in duplicates and only average results were reported in the figure. The figure clearly shows that the removal efficiency of both metals increased dramatically between 5 and 30 min, after which insignificant increases were noticed until 120 min. After 120 min, the removal efficiency of both metals was found to almost reach equilibrium. The rapid adsorption within the first 30 min could be attributed to the availability of surface area and active sites on the surface of the produced AC, where metal ions are adsorbed quickly to more active sites. Once available sites are filled, adsorption process becomes slower until saturation is reached. Based on the results, the equilibrium time was selected as 120 min, where adsorbed molecules of metal ions are equal to desorbing ones. At equilibrium time, maximum removal efficiencies of 34.5 and 63% for  $\text{Cd}^{2+}$  and  $\text{Pb}^{2+}$ , respectively, were obtained. Higher removal efficiencies of  $\text{Pb}^{2+}$  when compared to  $\text{Cd}^{2+}$  can be attributed to the above-mentioned reasons. Similar findings were reported by Seco et al. [36] and Kobya et al. [37] who studied the removal of  $\text{Cd}^{2+}$  and  $\text{Pb}^{2+}$  by treated pinus pinaster bark and AC from different agricultural waste, respectively. Moreover, Taty-Costodes et al. [33] investigated the effect of contact time on the removal efficiency of cadmium and lead. They reported that equilibrium time was reached in 20 min, however contact time of 120 min was maintained for all experiments in order to make sure that equilibrium is reached. In the current investigation, contact time was selected as 180 min for the same reasons given above.

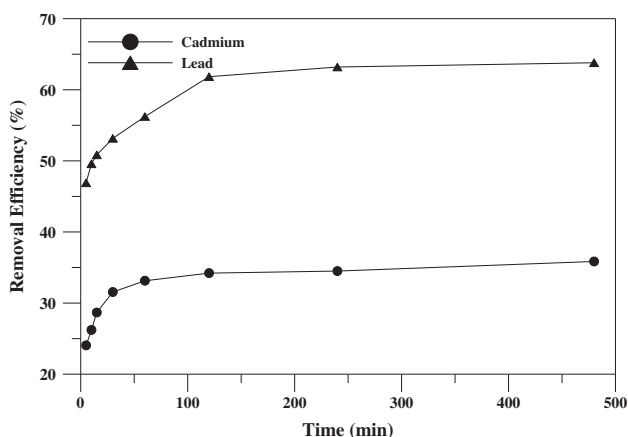


Fig. 5. Effect of contact time on adsorption of  $\text{Cd}^{2+}$  and  $\text{Pb}^{2+}$  using produced AC.

### 3.2.3. Effect of Initial concentration

To investigate the effect of initial concentration on the removal efficiency of  $\text{Cd}^{2+}$  and  $\text{Pb}^{2+}$  using the produced AC, adsorption isotherms were carried out at initial concentrations of 25, 50, 100, 200, and 300 mg/L, contact time of 180 min, pH value of 5, and adsorbent dosage of 50 mg per 50 mL of solution. The effect of initial concentration on the removal efficiency of  $\text{Cd}^{2+}$  and  $\text{Pb}^{2+}$  is depicted in Fig. 6. The results revealed that when initial concentration was increased from 25 to 300 mg/L, removal efficiencies of  $\text{Cd}^{2+}$  and  $\text{Pb}^{2+}$  decreased from 72 to 20%, and from 98 to 30%, respectively. The results also showed that removal efficiencies were found to decrease progressively when the initial concentration was increased from 25 to 150 mg/L, however, further increases in the initial concentration led to insignificant decrease in metals removal efficiencies. Seco et al. [36], who investigated removal of metals using granular AC, reported that metal removal can be attributed to the fact that produced AC surface contains definite number of high-energy sites. Therefore, at low concentrations, adsorption occurred at high-energy sites and when metal concentrations were increased, these sites became saturated. Consequently, metal ions were adsorbed to low-energy sites where energy of removal was decreased. On the other hand, the results showed that adsorption capacity was found to increase with the increase in initial concentrations of  $\text{Cd}^{2+}$  and  $\text{Pb}^{2+}$ . Adsorption capacities of  $\text{Cd}^{2+}$  and  $\text{Pb}^{2+}$  were found to increase from 18 to 56 mg/g and from 24.5 to 90 mg/g, respectively, when initial concentrations were increased from 25 to 300 mg/L. The increase in initial concentrations of  $\text{Cd}^{2+}$  and  $\text{Pb}^{2+}$  may have led to an increase in the

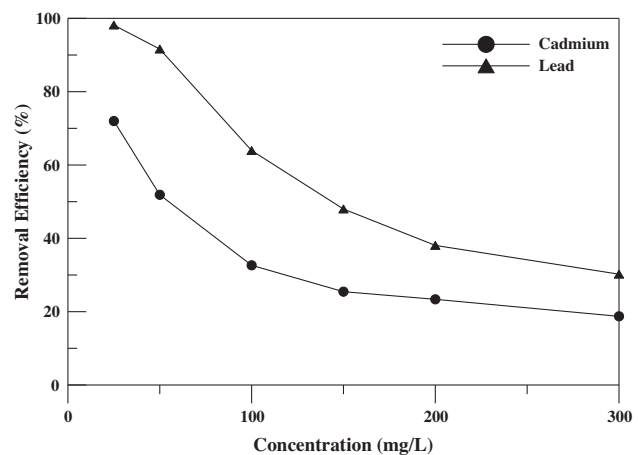


Fig. 6. Effect of metal concentration on adsorption of  $\text{Cd}^{2+}$  and  $\text{Pb}^{2+}$  using produced AC.

driving force, which in turn resulted in overcoming the mass transfer between solid and liquid phases. Moreover, increasing metal concentrations may have led to an increase in the interaction between the produced AC and metal ions. Similar results were reported by Taty-Costodes et al. [33] and Thajeel et al. [38] who investigated removal of metals using AC produced from sawdust and rice husk, respectively.

### 3.2.4. Effect of adsorbent dosage

To investigate the effect of dosage of the produced AC on the removal efficiency of  $\text{Cd}^{2+}$  and  $\text{Pb}^{2+}$ , adsorption isotherms were conducted using AC dosages of 25, 50, 100, 200, and 300 mg per 50 mL, initial concentrations of 100 mg/L, contact time of 180 min, and pH value of 5. Fig. 7 shows the effect of AC dosage on the removal efficiency of  $\text{Cd}^{2+}$  and  $\text{Pb}^{2+}$ . The figure clearly shows that the removal efficiency of both metals was initially increasing with the increase in dosage of the produced AC until it reached a stage after which insignificant increases in removal efficiencies were noticed. For  $\text{Cd}^{2+}$ , the removal efficiency increased from 21 to 78% when the AC dosage was increased from 25 to 200 mg per 50 mL (0.326% per mg AC). However, when the AC dosage was further increased to 300 mg per 50 mL, the removal efficiency was found to reach 85% (0.07% per mg AC). Similarly,  $\text{Pb}^{2+}$  removal efficiency was found to increase from 36 to 94% when the AC dosage was increased from 25 to 200 mg per 50 mL (0.331% per mg AC). When AC dosage was further increased to 300 mg per 50 mL, the removal efficiency was found to increase to 98% (0.04% per mg AC). This can be attributed to the fact that by increasing the adsorbent dosage, the AC sur-

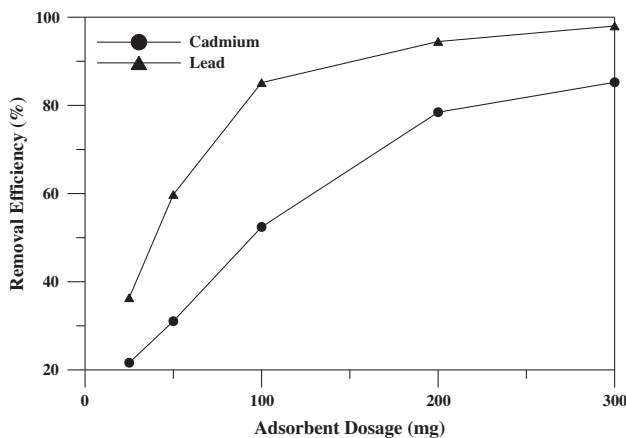


Fig. 7. Effect of adsorbent dosage on adsorption of  $\text{Cd}^{2+}$  and  $\text{Pb}^{2+}$  using produced AC.

face area as well as adsorption sites will increase, which will result in enhancing the removal efficiency of both metals. However, when the AC dosage was further increased, insignificant increase in the removal efficiency was achieved, which can be attributed to the attainment of equilibrium between the residual concentration of metal ions in the solution and surface metal ions concentration. These results are in agreement with those reported by Srivastava et al. [39] who studied adsorption behavior of toxic metals using AC produced from coconut. On the other hand, adsorption capacity was found to decrease with the increase in AC dosages of  $\text{Cd}^{2+}$  and  $\text{Pb}^{2+}$ , where adsorption capacity decreased from 43 to 14 and from 72 to 16 mg/g when AC dosages increased from 25 to 300, respectively. At lower adsorbent dosages, all adsorption sites become saturated, therefore, metal adsorption per gram of the produced AC is high. However, with increasing the AC dosage, unsaturated adsorption sites increase, thereby metal adsorption per AC gram decreases [40]. Onundi et al. [41] who used AC produced from palm shell for the removal of Pb and Ni from synthetic solutions reported that decrease of adsorption capacities could be caused by the overlapping of adsorption sites as a result of overcrowding of AC particles. Kumar and Gayathri [42], who investigated the removal of Pb using powder of bael tree leaf, reported similar findings.

### 3.3. Adsorption isotherms of $\text{Cd}^{2+}$ and $\text{Pb}^{2+}$

Eq. (2), which represents the linear form of Langmuir adsorption isotherm, was used to plot the relationship between metal concentration in solid phase ( $q_e$ ) and that in liquid phase ( $C_e$ ) at different initial concentrations of  $\text{Cd}^{2+}$  and  $\text{Pb}^{2+}$ .

$$(C_e/q_e) = \frac{1}{K_L} + \frac{a_L}{K_L} \times C_e \quad (2)$$

Fig. 8 shows Langmuir adsorption isotherm of  $\text{Cd}^{2+}$  and  $\text{Pb}^{2+}$ , where good fitting was observed with correlation coefficient ( $R^2$ ) of 0.95 and 0.98, respectively. Table 4 shows that maximum adsorption capacities ( $Q_0$ ) were 61 and 90 mg/g for  $\text{Cd}^{2+}$  and  $\text{Pb}^{2+}$ , respectively.

Moreover, Eq. (3) that represents the linear form of Freundlich isotherm was used to plot obtained data on adsorption capacities at different concentrations of  $\text{Cd}^{2+}$  and  $\text{Pb}^{2+}$ .

$$\log q = \log K_F + \frac{1}{n} \log C \quad (3)$$

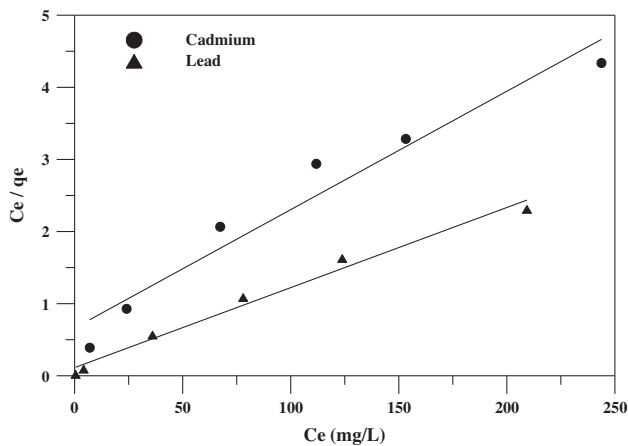


Fig. 8. Langmuir isotherm of  $\text{Cd}^{2+}$  and  $\text{Pb}^{2+}$  adsorption using produced AC.

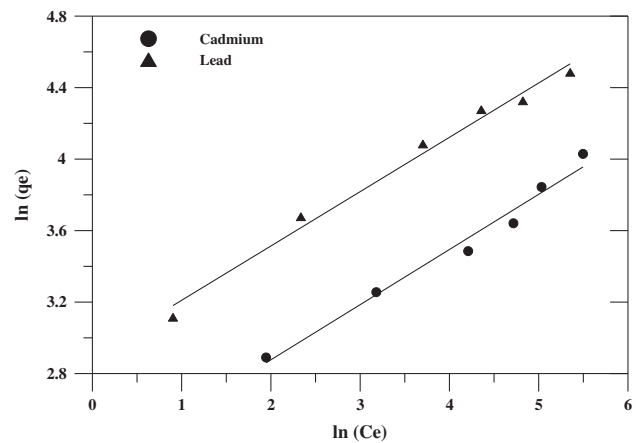


Fig. 9. Freundlich isotherm of  $\text{Cd}^{2+}$  and  $\text{Pb}^{2+}$  adsorption using produced AC.

Fig. 9 clearly indicates the good fitting with correlation coefficient ( $R^2$ ) of 0.98 and 0.99 for  $\text{Cd}^{2+}$  and  $\text{Pb}^{2+}$ , respectively. The affinity in Freundlich isotherm is non-uniform over the surface of the adsorbent and each site on the adsorbent surface has different affinity, which means adsorption of both metals occurs as multilayers on heterogeneous surface of the produced AC. Mohan and Chander [43], who investigated the removal of Cd using AC produced from bagasse, reported similar results. Moreover, similar results were reported by Depci et al. [44] who studied competitive adsorption of Pb and Zn on AC produced from Van apple pulp. The Isotherm parameters are summarized in Table 4 where values of  $n$  ( $n = 3.24$ – $3.3$ ) indicate good adsorption characteristics. According to Aksu and Kutsal [45] who studied the removal of Pb from wastewater, adsorption characteristics based on  $n$  values are classified as good ( $n$  from 2 to 10), relatively good ( $n$  from 1 to 2), and poor ( $n < 1$ ).

Table 4  
Parameters of Langmuir and Freundlich isotherms

Isotherm parameter	$\text{Cd}^{2+}$	$\text{Pb}^{2+}$
<i>Langmuir</i>		
$K_L$ (L/g)	1.521	8.894
$a_L$ (L/mg)	0.025	0.099
$Q_0$ (mg/g)	60.90	90.10
$R^2$	0.95	0.98
<i>Freundlich</i>		
$K_F$ (mg/g)	9.587	19.181
$n$	3.24	3.30
$R^2$	0.978	0.987

### 3.4. Adsorption kinetic model of $\text{Cd}^{2+}$ and $\text{Pb}^{2+}$

The experimental data of  $\text{Cd}^{2+}$  and  $\text{Pb}^{2+}$  were fitted to the following linear pseudo-first-order model:

$$\log(q_e - q_t) = \log(q_e) - \frac{K_1}{2.303} \times t \quad (4)$$

where  $q_e$  is the equilibrium adsorption capacity (mg/g),  $q_t$  is the adsorption capacity at time  $t$  (mg/g), and  $K_1$  is the pseudo-first-order constant rate (per minute). Fig. 10 shows the pseudo-first-order plot for  $\text{Cd}^{2+}$  and  $\text{Pb}^{2+}$  adsorption, where the value of  $\log(q_e - q_t)$  was plotted against time. Table 5 clearly shows that although the correlation coefficient ( $R^2$ ) was 0.98 for both  $\text{Cd}^{2+}$  and  $\text{Pb}^{2+}$ , theoretical values of  $q_e$  (9.78 and 18.18 mg/g) are not in good agreement with experimental ones (34.5–63.20 mg/g). Therefore, it can be concluded that results of both metals adsorption kinetics do not follow a pseudo-first-order kinetic model. Similar results were reported by Taty-Costodes et al. [33] who investigated kinetic models for the removal of Cd using AC produced from sawdust. Consequently, the experimental results of both metals were fitted to the following pseudo-second-order model:

$$\frac{t}{q_t} = \frac{1}{K_2 q_e^2} + \frac{1}{q_e} \times t \quad (5)$$

where  $K_2$  is pseudo-second-order constant rate (g/mg min). From the plot shown in Fig. 11, the parameters of this model  $K_2$  and  $q_e$  were determined from the slope and the  $y$ -intercept of the plots. Table 5 clearly shows the agreement of the experimental and

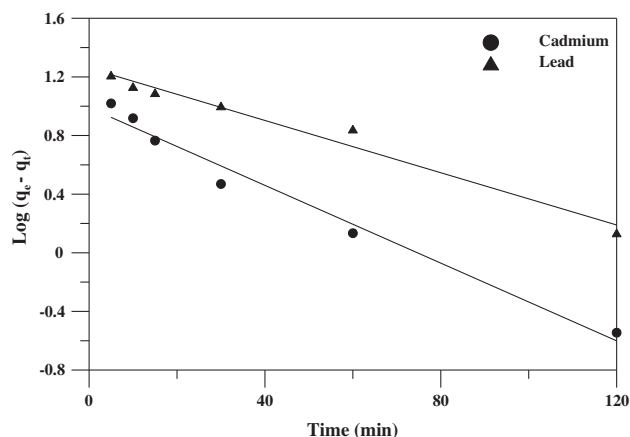


Fig. 10. Pseudo-first-order kinetic adsorption model of  $\text{Cd}^{2+}$  and  $\text{Pb}^{2+}$  adsorption.

Table 5  
Pseudo-first and second order parameters for cadmium and lead adsorption

Parameter	Pseudo-second-order		Pseudo-first-order	
	$\text{Pb}^{2+}$	$\text{Cd}^{2+}$	$\text{Pb}^{2+}$	$\text{Cd}^{2+}$
$R^2$	0.998	0.999	0.98	0.98
$K$	0.003	0.006	0.021	0.031
Theoretical $q_e$ (mg/g)	64.36	35.90	18.18	9.78
Experimental $q_e$ (mg/g)	63.20	34.50	63.20	34.50

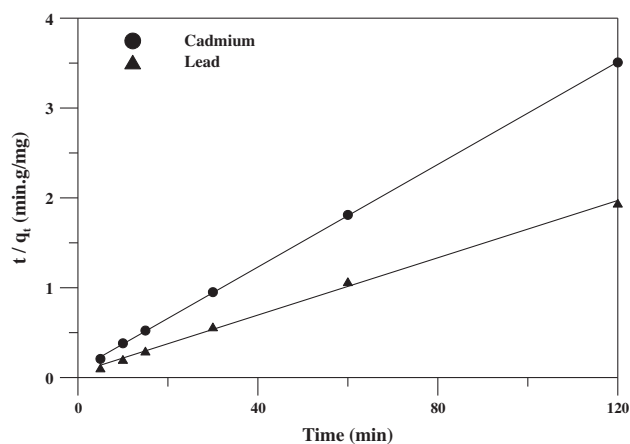


Fig. 11. Pseudo-second-order kinetic adsorption model of  $\text{Cd}^{2+}$  and  $\text{Pb}^{2+}$  adsorption.

calculated values of  $q_e$ . As a result, it can be concluded that the adsorption process of  $\text{Cd}^{2+}$  and  $\text{Pb}^{2+}$  follows a pseudo-second-order kinetic model, which suggests a chemical adsorption including electron

exchange between the produced AC and both metals. Similar findings were reported by Bohli et al. [34] and Mohan et al. [46], who studied kinetic models of Cd removal by AC derived from wood and olive stone, respectively. Moreover, Depci et al. [44], who investigated the removal of Pb from single and competitive solutions by AC produced from Van apple pulp, reported results that are in agreement with those reported in the current research.

#### 4. Conclusions

In conclusion, MOSW was exploited as a low-cost source of AC, which was produced at optimum conditions of carbonization temperature and time and phosphoric acid ( $\text{H}_3\text{PO}_4$ ) concentration as an activation agent. Surface characteristics of MOSW and produced AC were investigated using BET, SEM, XRD, and FT-IR. The produced AC was exploited as adsorbent for the removal of heavy metals ( $\text{Cd}^{2+}$  and  $\text{Pb}^{2+}$ ) from synthetic industrial wastewater through adsorption isotherm experiments. The effect of operational factors such as contact time, pH, metal concentration, and adsorbent dosage on the adsorption performance was investigated. Results on maximum removal efficiencies indicated that  $\text{Pb}^{2+}$  has more affinity to the produced AC than  $\text{Cd}^{2+}$ , which was attributed to electronegativity, ionic radius, and hydrated ionic radius. The experimental data of adsorption was fitted to Langmuir and Freundlich isotherms, where better fittings were observed with Freundlich isotherm. The affinity in Freundlich isotherm is non-uniform over the surface of the adsorbent and each site on the adsorbent surface has different affinity, which means adsorption of both metals ( $\text{Cd}^{2+}$  and  $\text{Pb}^{2+}$ ) occurs as multilayers on heterogeneous surface of the produced AC. The isotherms also showed that the maximum adsorption capacity of  $\text{Pb}^{2+}$  was higher than that of  $\text{Cd}^{2+}$ , which was attributed to the same above-mentioned reasons. The experimental data of adsorption was also fitted to pseudo-first-order and pseudo-second-order kinetic models. The results showed that pseudo-second-order kinetic model was found to be followed, which suggest chemical adsorption including electron exchange between metals ( $\text{Cd}^{2+}$  and  $\text{Pb}^{2+}$ ) and the produced AC.

#### Acknowledgment

The authors would like to express their gratitude to King Fahd University of Petroleum & Minerals (Dhahran, Saudi Arabia) for financial and technical supports provided throughout the research period.

## References

- [1] M.M. Rahman, M. Adil, A.M. Yusof, Y.B. Kamaruzzaman, R.H. Ansary, Removal of heavy metal ions with acid activated carbons derived from oil palm and coconut shells, *Materials* 7 (2014) 3634–3650.
- [2] C. Wong, J.P. Barford, G. Chen, G. McKay, Kinetics and equilibrium studies for the removal of cadmium ions by ion exchange resin, *J. Environ. Chem. Eng.* 2 (2014) 698–707.
- [3] M. Kobya, N. Erdem, E. Demirbas, Treatment of Cr, Ni, and Zn from galvanic rinsing wastewater by electrocoagulation process using iron electrodes, *Desalin. Water Treat.* 56 (2015) 1191–1201.
- [4] P. Ghosh, A.N. Samanta, S. Ray, Reduction of COD and removal of  $Zn^{2+}$  from rayon industry wastewater by combined electro-Fenton treatment and chemical precipitation, *Desalination* 266 (2011) 213–217.
- [5] Y. Cui, Q. Ge, X.Y. Liu, T. Chung, Novel forward osmosis process to effectively remove heavy metal ions, *J. Membr. Sci.* 467 (2014) 188–194.
- [6] M.A. Barakat, New trends in removing heavy metals from industrial wastewater, *Arabian J. Chem.* 4 (2011) 361–377.
- [7] D. Mohan, A. Sarswat, Y.S. Ok, C.U. Pittman, Organic and inorganic contaminants removal from water with biochar, a renewable, low cost and sustainable adsorbent—A critical review, *Bioresour. Technol.* 160 (2014) 191–202.
- [8] K. Kadirvelu, K. Thamaraisel, C. Namasivayam, Removal of heavy metals from industrial wastewaters by adsorption onto activated carbon prepared from an agricultural solid waste, *Bioresour. Technol.* 76 (2001) 63–65.
- [9] F. Wu, R. Tseng, Preparation of highly porous carbon from fir wood by KOH etching and  $CO_2$  gasification for adsorption of dyes and phenols from water, *J. Colloid Interface Sci.* 294 (2006) 21–30.
- [10] L. Muniandy, F. Adam, A.R. Mohamed, E. Ng, The synthesis and characterization of high purity mixed microporous/mesoporous activated carbon from rice husk using chemical activation with NaOH and KOH, *Microporous Mesoporous Mater.* 197 (2014) 316–323.
- [11] J. Shou, M. Qiu, Adsorption kinetics of phenol in aqueous solution onto activated carbon from wheat straw lignin, *Desalin. Water Treat.* 57 (2016) 3119–3124, doi: [10.1080/19443994.2014.983983](https://doi.org/10.1080/19443994.2014.983983).
- [12] M.E. Fernandez, G.V. Nunell, P.R. Bonelli, A.L. Cukierman, Activated carbon developed from orange peels: Batch and dynamic competitive adsorption of basic dyes, *Ind. Crops Prod.* 62 (2014) 437–445.
- [13] H. Gupta, B. Gupta, Adsorption of polycyclic aromatic hydrocarbons on banana peel activated carbon, *Desalin. Water Treat.* 1–12, doi: [10.1080/19443994.2015.1029007](https://doi.org/10.1080/19443994.2015.1029007).
- [14] M.A. Ahmad, N.A. Puad, O.S. Bello, Kinetic, equilibrium and thermodynamic studies of synthetic dye removal using pomegranate peel activated carbon prepared by microwave-induced KOH activation, *Water Res. Ind.* 6 (2014) 18–35.
- [15] C.S. Mahajan, R.N. Sarode, S.B. Jadhav, S.T. Attarde, Ingle, removal of heavy metals from winery wastewater by using natural adsorbents, *Int. J. Conserv. Sci.* 5 (2014) 69–78.
- [16] F. Gönen, D.S. Serin, Adsorption study on orange peel: Removal of Ni(II) ions from aqueous solution, *African J. Biotechnol.* 11 (2012) 1250–1258.
- [17] G. Annadural, R.S. Juang, D.J. Lee, Adsorption of heavy metals from water using banana and orange peels, *Water Sci. Technol.* 47 (2003) 185–190.
- [18] K. Kadirvelu, M. Kavipriya, C. Karthika, M. Radhika, N. Vennilamani, S. Patabhi, Utilization of various agricultural wastes for activated carbon preparation and application for the removal of dyes and metal ions from aqueous solutions, *Bioresour. Technol.* 87 (2003) 129–132.
- [19] E. El-Ashtoukhy, N. Amin, O. Abdelwahab, Removal of lead (II) and copper (II) from aqueous solution using pomegranate peel as a new adsorbent, *Desalination* 223 (2008) 162–173.
- [20] T. Aman, A.A. Kazi, M.U. Sabri, Q. Bano, Potato peels as solid waste for the removal of heavy metal copper (II) from waste water/industrial effluent, *Colloids Surf. B* 63 (2008) 116–121.
- [21] M.A. Habila, Z.A. AlOthman, R. Ali, A.A. Ghafar, M.S.E.-D. Hassouna, Removal of tartrazine dye onto mixed-waste activated carbon: kinetic and thermodynamic studies, *Clean—Soil Air Water* 42 (2014) 1824–1831.
- [22] E. Leimkuehler, Production, Characterization, and Applications of Activated Carbon, M.Sc Thesis, University of Missouri, Missouri, 2010.
- [23] S. Brunauer, P.H. Emmett, E. Teller, Adsorption of gases in multimolecular layers, *J. Am. Chem. Soc.* 60 (1938) 309–319.
- [24] A. El-Hendawy, A.J. Alexander, R.J. Andrews, G. Forrest, Effects of activation schemes on porous, surface and thermal properties of activated carbons prepared from cotton stalks, *J. Anal. Appl. Pyrolysis* 82 (2008) 272–278.
- [25] A. El-Hendawy, Variation in the FT-IR spectra of a biomass under impregnation, carbonization and oxidation conditions, *J. Anal. Appl. Pyrolysis* 75 (2006) 159–166.
- [26] B.S. Girgis, E. Smith, M.M. Louis, A. El-Hendawy, Pilot production of activated carbon from cotton stalks using  $H_3PO_4$ , *J. Anal. Appl. Pyrolysis* 86 (2009) 180–184.
- [27] T. Liou, Development of mesoporous structure and high adsorption capacity of biomass-based activated carbon by phosphoric acid and zinc chloride activation, *Chem. Eng. J.* 158 (2010) 129–142.
- [28] W. Tongpoothorn, M. Sriuttha, P. Homchan, S. Chanthai, C. Ruangviriyachai, Preparation of activated carbon derived from *Jatropha curcas* fruit shell by simple thermo-chemical activation and characterization of their physico-chemical properties, *Chem. Eng. Res. Des.* 89 (2011) 335–340.
- [29] S. Salehin, A.S. Aburizaiza, M.A. Barakat, Activated carbon from residual oil fly ash for heavy metals removal from aqueous solution, *Desalin. Water Treat.* 57 (2016) 278–287.
- [30] Y. Li, Z. Di, J. Ding, D. Wu, Z. Luan, Y. Zhu, Adsorption thermodynamic, kinetic and desorption studies of  $Pb^{2+}$  on carbon nanotubes, *Water Res.* 39 (2005) 605–609.
- [31] Y. Örkün, N. Karatepe, R. Yavuz, Influence of temperature and impregnation ratio of  $H_3PO_4$  on the production of activated carbon from hazelnut shell, *Acta Phys. Pol. A.* 121 (2012) 277–280.

- [32] M.A. Atieh, O.Y. Bakather, B.S. Tawabini, A.A. Bukhari, M. Khaled, M. Alharthi, M. Fettouhi, F.A. Abuilaiwi, Removal of chromium (III) from water by using modified and nonmodified carbon nanotubes, *J. Nanomaterials* 2010 (2010) 1–9 (Article ID 232378).
- [33] V.C. Taty-Costodes, H. Fauduet, C. Porte, A. Delacroix, Removal of Cd(II) and Pb(II) ions, from aqueous solutions, by adsorption onto sawdust of *Pinus sylvestris*, *J. Hazard. Mater.* 105 (2003) 121–142.
- [34] T. Bohli, A. Ouederni, N. Fiol, I. Villaescusa, Evaluation of an activated carbon from olive stones used for heavy metal removal from aqueous phase, *C.R. Chim.* 18 (2015) 88–99.
- [35] F. Qin, B. Wen, X.Q. Shan, Y.N. Xie, T. Liu, S.Z. Zhang, S.U. Khan, Mechanisms of competitive adsorption of Pb, Cu, and Cd on peat, *Environ. Pollut.* 144 (2006) 669–680.
- [36] A. Seco, C. Gabaldón, P. Marzal, A. Aucejo, Effect of pH, cation concentration and sorbent concentration on cadmium and copper removal by a granular activated carbon, *J. Chem. Technol. Biotechnol.* 74 (1999) 911–918.
- [37] M. Kobya, E. Demirbas, E. Senturk, M. Ince, Adsorption of heavy metal ions from aqueous solutions by activated carbon prepared from apricot stone, *Biore-sour. Technol.* 96 (2005) 1518–1521.
- [38] A.S. Thajeel, M.M. Al-Faize, A.Z. Raheem, Adsorption of  $Pb^{+2}$  and  $Zn^{+2}$  ions from oil wells onto activated carbon produced from rice husk in batch adsorption process, *J. Chem. Pharm. Res.* 5 (2013) 240–250.
- [39] V.C. Srivastava, I.D. Mall, I.M. Mishra, Adsorption of toxic metal ions onto activated carbon, *Chem. Eng. Process.* 47 (2008) 1269–1280.
- [40] M.M. Rao, D.K. Ramana, K. Seshiah, M.C. Wang, S.W.C. Chien, Removal of some metal ions by activated carbon prepared from *Phaseolus aureus* hulls, *J. Hazard. Mater.* 166 (2009) 1006–1013.
- [41] Y.B. Onundi, A.A. Mamun, M.F. Al Khatib, Y.M. Ahmed, Adsorption of copper, nickel and lead ions from synthetic semiconductor industrial wastewater by palm shell activated carbon, *Int. J. Environ. Sci. Technol.* 7 (2010) 751–758.
- [42] P.S. Kumar, R. Gayathri, Adsorption of  $Pb^{2+}$  ions from aqueous solutions onto bael tree leaf powder: Isotherms, kinetics and thermodynamics study, *J. Eng. Sci. Technol.* 4 (2009) 381–399.
- [43] D. Mohan, S. Chander, Single component and multi-component adsorption of metal ions by activated carbons, *Colloids Surf. A* 177 (2001) 183–196.
- [44] T. Depci, A.R. Kul, Y. Önal, Competitive adsorption of lead and zinc from aqueous solution on activated carbon prepared from Van apple pulp: Study in single- and multi-solute systems, *Chem. Eng. J.* 200–202 (2012) 224–236.
- [45] Z. Aksu, T. Kutsal, A bioseparation process for removing lead (II) ions from waste water by using *C. vulgaris*, *J. Chem. Technol. Biotechnol.* 52 (1991) 109–118.
- [46] D. Mohan, C.U. Pittman, M. Bricka, F. Smith, B. Yancey, J. Mohammad, P.H. Steele, M.F. Alexandre-Franco, V. Gómez-Serrano, H. Gong, Sorption of arsenic, cadmium, and lead by chars produced from fast pyrolysis of wood and bark during bio-oil production, *J. Colloid Interface Sci.* 310 (2007) 57–73.